



Adapted Single Scale Retinex Algorithm for Nighttime Image Enhancement Mohammad Khalil Ismail, Zohair Al-Ameen *

Department of Computer Science, College of Computer Science and Mathematics, University of Mosul, Mosul, Nineveh, Iraq

*Corresponding author. Email: qizohair@uomosul.edu.iq

Article information

Article history:

Received : 24/10/2021
Accepted : 29/11/2021
Available online :

Abstract

Images captured at night with low-light conditions frequently have a loss of visible details, inadequate contrast, low brightness, and noise. Therefore, it is difficult to perceive, extract, and analyze important visual information from these images, unless they were properly processed. Different algorithms exist to process nighttime images, yet most of these algorithms are highly complex, generate processing artifacts, over-smooth the images, or do not improve the illumination adequately. Thus, the single scale retinex (SSR) algorithm is adopted in this study to provide better processing for nighttime images. The proposed algorithm starts by converting the color image from the RGB model to the HSV model and enhancing the V channel only while preserving the H and S channels. Then, it determined the image's illuminated version somewhat like the SSR, computes the logarithms of the illuminated and original images, then subtracts these two images by utilizing an altered procedure. Next, a modified gamma-adjusted Rayleigh distribution function is applied, and its outcome is processed once more by an automatic linear contrast stretching approach to produce the processed V channel that will be utilized with the preserved H and S channels to generate the output RGB image. The developed algorithm is assessed using a real dataset of nighttime images, evaluated using three dedicated image evaluation methods, and compared to ten dissimilar contemporary algorithms. The obtained results demonstrated that the proposed algorithm can significantly improve the perceptual quality of nighttime images and suppress artifact generation rapidly and efficiently, in addition to showing the ability to surpass the performance of different existing algorithms subjectively and objectively.

Keywords:

Image enhancement, Nighttime image, Single scale retinex, Statistical methods, SSR, HSV.

Correspondence:

Author Zohair Al-Ameen
Email: qizohair@uomosul.edu.iq

I. INTRODUCTION

Recently, the topic of nighttime image enhancement has attracted broad interest since taking nighttime images increased dramatically to visualize broad night events, in that nighttime images usually contain compressed dynamic range, low contrast, poor visibility, and random noise [1]. To tackle such an issue, various image enhancement (IE) techniques have been introduced to help in improving the quality of digital images by providing actual processing using arithmetical, statistical, and logical approaches [2].

The main goal of IE is to well-improve the visual perception of digital images without generating undesirable effects that can affect the important information in the processed image [3]. IE methods are useful for generating new images from the originals with better-viewed details. Thus, contrast modification, illumination enhancement, sharpening, and spatial filtering are among the most popular techniques of IE [4]. Besides, computer vision and multimedia algorithms require images with high visibility. However, images that were taken in low-light conditions

such as nighttime images often have low visibility, poor illumination, and inadequate details presentation [5]. Therefore, the need to enhance such images before further processing is highly required. Samples of different nighttime images are given in Figure 1.



Fig. 1. Samples of different nighttime images.

In general, IE techniques can make the input images look better and be more suitable for specific applications [6]. However, improving the visibility of low illumination images requires the consideration of three major issues. The first is to maintain the significant image information without introducing distortions, the second is to increase the illumination in the dark areas, preserve the illumination from being extremely amplified in the bright areas, and provide sufficient contrast and adequate colors. The third is to preserve image sharpness and prevent the over-smoothing effect [7-10]. The Retinex theory has been used in many research works to process nighttime images.

It has three classical algorithms which are the multi-scale retinex with color restoration (MSRCR), multi-scale retinex (MSR), and single scale retinex (SSR) [11]. However, the latter is the simplest in structure and computations, and its standard versions did not ensure proper output in terms of color representation and tonal distribution. The MSR on the other hand ensured these two traits, but it could not produce proper colorfulness as it utilized a linear weighting procedure for the scales. The MSRCR could attain much better colorfulness, but it was not successful when applied in a real-time mode due to the need for numerous parameters to be set properly. Likewise, these algorithms produced some degradations like color distortions and halo artifacts in the image areas that own high contrast due to the use of a Gaussian filter to get the illuminated image [12].

In addition, many methods have been introduced in the past years for nighttime image enhancement, wherein a sufficient review of such methods is given in section 2 of this study. This research aims at developing the SSR algorithm to process different nighttime images rapidly and efficiently. Mathematical and statistical methods are utilized to adapt the SSR algorithm to the nature of nighttime images. Besides, a newly generated dataset of real nighttime images is used in this research, which is generated using cameras like Nikon D750 and Samsung A70 smartphone. The adapted SSR algorithm is compared with various advanced and contemporary algorithms that were explained in the literature review to know the real

capabilities of the adapted algorithm. Analysis and discussions are given to explain the reached findings. The rest of this article is ordered as follows: Section II reviews different legacy methods; Section III explains the retinex theory, the standard SSR, and the proposed algorithm; Section IV explains the topic of image evaluation and the methods used in this study; Section V provides the experimental and comparison results accompanied by the required analysis and interpretation of findings; Section VI describes the important reached remarks as a conclusion.

II. RELATED WORK

Researchers have worked hard in the past years to develop specialized methods that can process nighttime images efficiently using the retinex theory and other processing concepts. In [13], the authors introduced an improved MSR (IMSR) algorithm, which starts by computing various scales of the gaussian filter and applying them to the input image. Then, calculate the lightness ratio between the input image and the results of the previous step. Next, compute the sigmoid of ratios and determine their mean value. After that, determine the weights based on the computations of the first step. Finally, apply the addition process by utilizing the determined weight to get the output image. Besides, the authors developed a probabilistic-based image enhancement (PIE) method in [14], which starts by inputting the image with four adjustment parameters and two stopping parameters. Next, a maximum a posteriori (MAP) procedure is applied to get the reflectance image and the illuminated image. Then, an iterative approach is followed which includes direction alternation to solve the MAP issues to provide the output.

In [15], the authors proposed a fusion-based enhancement (FBE) algorithm, which starts by applying a morphological closing process to get the reflectance and illumination images from the input image. Then, from the illumination image, two images are obtained that represent its contrast and illumination improved observations using improved histogram equalization and sigmoid approaches. Next, two weights are determined depending on the two improved observations and a multiscale fusion process is applied to produce the adjusted image which will be used later by compensating it back to the reflectance image to get the output. Moreover, the authors created an algorithm that depends on the camera response model (CRM) in [16]. It starts by estimating the CRM and exposure ratio map (ERM). By taking advantage of the histogram features of CRM and ERM, the exposure of the input image is adjusted followed by the estimation of a more accurate ERM using different luminance approximation methods. Using aforesaid information, the CRM is refined, the enhancement is applied, and the output of the algorithm is obtained.

In [17], the authors developed an algorithm named low-light image enhancement (LIME), which starts by receiving the input image along with some parameters. Then, the

weighting matrix is created followed by the approximation of the primary illumination map. Next, this illumination map is refined using different solvers. Next, a gamma-correction technique is applied to adjust the illumination and contrast. The output is then checked for noise existence, and if the high ratios of noise were detected, a specialized denoising approach is applied and the algorithm's output is created. In addition, the authors introduced a light enhancement with a camera response model (LEARM) based algorithm in [18], which starts by inputting an image and the threshold value. Then, a specific CRM is selected, and its parameters are determined. Next, a sped-up solver is applied to obtain the illumination map followed by determining the ERM using a specific approach. The output image is obtained by using the predetermined and inputting values using a dedicated specialized equation.

In [19], the authors proposed an algorithm named LightenNet that utilizes the concepts of retinex theory convolution neural network (CNN). It starts by receiving the input image then it utilizes the CNN to extract and improve the illumination of features followed by non-linear mapping and reconstruction to get the illumination image. Next, the retinex theory is applied to further improve the illumination and produce the output. Furthermore, the authors developed a fractional-order fusion model (FOFM) based algorithm in [20], which starts by estimating the reflectance and illumination images from the input image. Then, these two versions are enhanced using a designated CRM model to produce the first enhanced image. Next, the reflectance and illumination images are determined for the first enhanced image and enhanced using another designated CRM model to produce a second enhanced image. At this point, three images are available which are the original, the first enhanced, and the second enhanced. Next, A multiscale fusion is done between these three images by utilizing Laplacian and gaussian pyramids to produce the algorithm's output.

In [21], the authors introduced an adaptive image enhancement (AIE) algorithm, which starts by converting the image from the RGB domain to the HSV domain. Then, the reflectance is estimated from the V channel. Next, an adaptive illumination enhancement procedure is applied to the V channel using logarithmic operations. Then, a multi-scale fusion process based on principal component analysis is applied to further enhance the image. The produced image in the HSV domain is converted back to the RGB domain to get the final output. Finally, the authors created a semi-decoupled decomposition (SDD) based algorithm in [22], which starts by receiving the degraded image with 8 other parameters as an input. Next, an iterative process starts by semi-decoupling the image into its reflectance and illumination parts then improves the illumination part using the retinex theory, specialized approaches, and total variation

denoising. The final output is obtained when the iterative process ends.

From the reviewed algorithms, a variety of concepts have been used previously to improve illumination. Still, the complexity is high, many inputs are required, including a denoising step that can introduce over smoothness, and some concepts do not produce sufficient illumination. Hence, the opportunity still stands to introduce a new method that has high capabilities to filter nighttime images adequately while avoiding the undesirable drawbacks of the previously developed algorithms.

III. RETINEX THEORY

The Retinex theory was proposed by Edwin H. Land in the year 1963. It is an abbreviation of two words including retina and cortex. The aim of using this theory is to clarify how human beings perceive the illumination and colors of an object. Retinex theory assumes that the image in human eyes can be produced by two factors which are illumination and reflection as shown in Figure 2. In this figure, it can be observed that the observed image can be decomposed into the brightness matrix produced by the light source and the reflectivity matrix of the object [23]. The Retinex theory was classified under the center-surround function. The output value of this function is determined by the input which represents the center and its neighborhood which represents the surrounding [24]. As known, different algorithms have been developed depending on the Retinex theory such as SSR, MSR, and MSRCR, with the SSR being the simplest in terms of computations [25]. In the next sub-section, the working mechanism of the SSR is given.

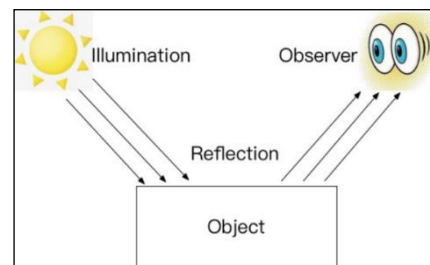


Fig. 2. Illustration of retinex theory [23].

3.1 Standard SSR Algorithm

In the SSR, the illumination is estimated by convolving (*) the discrete Gaussian surround function (DGSF) $G_{(x,y)}$ with the input image $I_{(x,y)}$. Then, compute the logarithms for both the degraded image and illumination images. To find the reflection image $R_{(x,y)}$, the log of the illumination image is subtracted from the log of a degraded image [26], in that $R_{(x,y)}$ signifies an improved version of $I_{(x,y)}$. The standard SSR algorithm is determined as follows:

- 1- Compute the DGSF as follows:

$$G_{(x,y)} = T \cdot \exp\left(-\frac{(A^2 + B^2)}{2\sigma^2}\right) \quad (1)$$

$$T = \frac{1}{\sum_{i=1}^N \sum_{j=1}^M \exp\left(-\frac{(A^2 + B^2)}{2\sigma^2}\right)} \quad (2)$$

where T is a normalization factor, x and y are the coordinates of the digital image; A and B signify two grayscale gradients in that the first one is horizontal and the other one is vertical, and they both have the same size as $I_{(x,y)}$. Moreover, M and N are image dimensions, and (\cdot) stands for a multiplication operator, while σ is a luminance controlling parameter.

2- Compute the SSR by the following equation:

$$R_{(x,y)} = \log\left[I_{(x,y)}\right] - \log\left[G_{(x,y)} * I_{(x,y)}\right] \quad (3)$$

where $R_{(x,y)}$ is the SSR output. The SSR treats reflectance as the final enhanced result. When applying the SSR to different nighttime images, the results look unnatural and introduced over-enhancement artifacts [27]. The standard SSR algorithm is applied to different nighttime images that are obtained by a Nikon D750 professional camera, and samples of the attained outcomes are shown in Figure 3.



Fig. 3. Output samples of the standard SSR when processing dissimilar nighttime images.

From Figure 3, it is noticed that the SSR has increased the luminosity but recorded some intrinsic disadvantages such as (1) the colors of the recovered images unnatural due to the amplification of the brightness in certain areas of the image, (2) loss of visual information due to the increased darkness in some areas of the processed image, (3) it introduced halo artifacts, and (4) it provided improper contrast and a total unusual look. Regardless of these drawbacks, the SSR was utilized for luminosity and contrast enhancement, and it has great potential for further development because it has shown the ability to be applied with the nighttime image including simple calculations [28]. The upcoming block diagram in Figure 4 explains the working mechanism of the SSR algorithm [29].

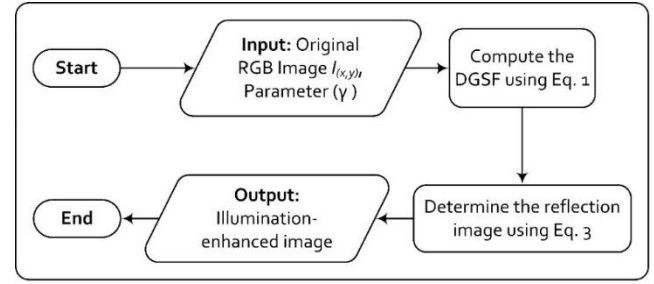


Fig. 4. Block diagram of the traditional SSR algorithm.

3.2 Proposed Adapted SSR Algorithm

The main purpose behind choosing the SSR algorithm is that many enhancements can be applied to it to improve its processing ability. In the developed algorithm, nighttime images are processed adequately with some simple procedures. The key purpose of creating the developed algorithm is to improve the visual details of nighttime images without introducing color distortions or over-enhancement artifacts. When dealing with nighttime images, the original SSR algorithm may show some flaws as mentioned earlier. Therefore, a new and low-intricacy algorithm has been introduced to process different nighttime images adequately depending on the SSR model and other processing concepts that are uncomplicated to produce better results.

The proposed adapted SSR (ASSR) algorithm is anticipated to process various nighttime images and produce results with improved illumination, adjusted contrast, and acceptable colors without introducing over-smoothness or processing flaws. The ASSR algorithm starts by converting the input RGB image to the hue saturation value color model (HSV). Since image illumination must be performed directly on RGB channels, it is difficult to ensure that all channels are enhanced in the correct ratio, which often results in color distortions after the correction process. All the hue, saturation, and intensity components of an image are independent when converted to the HSV model. As a result, changing the intensity values has little effect on the image's color. The RGB color model is transferred and transformed into an HSV model for this purpose [30], and in this algorithm, the processing happens on the value channel only. The second phase includes computing the DGSF by equations 1 and 2 using $\sigma = N \times M$. The third phase includes computing the luminance image by finding convolution (multiplication in the frequency domain with frequency shift then converting the results back to the spatial domain) between the original image and the result of the output of the previous step:

$$S_{(x,y)} = G_{(x,y)} \cdot V_{(x,y)} \quad (4)$$

where, $V_{(x,y)}$ is the value channel of the input image $I_{(x,y)}$. The fourth phase includes computing the log of $V_{(x,y)}$ and $S_{(x,y)}$ as follows:

$$O_{(x,y)} = \log [V_{(x,y)} + \varepsilon] \quad (5)$$

$$L_{(x,y)} = \log [S_{(x,y)} + \varepsilon] \quad (6)$$

where ($\varepsilon = 0.1$), in that ε is used to avoid having infinity values that come from calculating the log of zero. Then, the fifth phase is implemented by applying a new subtraction approach. In [44], the authors introduced a logarithmic approach to subtract two given images and create a new image $K_{(x,y)}$. In this work, a modified subtraction approach is employed instead of the subtraction method of the standard SSR which is given in Eq. 3. The original subtraction approach that was described in [31] is calculated using the following equation:

$$K_{(x,y)} = W \cdot \frac{(O_{(x,y)} - L_{(x,y)})}{W - L_{(x,y)}} \quad (7)$$

where W is a constant number, whose value is one (considering that the dynamic range is between 0 and 1). In this work, this equation is adapted so that it can be applied as the developed subtraction approach for this algorithm. The following equation is used to describe the adapted subtraction approach which will be applied in the developed algorithm:

$$K_{(x,y)} = \frac{(O_{(x,y)} - (L_{(x,y)})^2)}{-L_{(x,y)}} \quad (8)$$

where $K_{(x,y)}$ represents the image reflection. The output of this step needs further contrast and illumination enhancements. Thus, the sixth phase is implemented by applying an altered counterpart of the CDF of Rayleigh distribution to modify the contrast of the reflection image. The CDF of Rayleigh distribution is deemed an S-shape transform which was utilized in different research works related to contrast and illumination enhancements [32]. The CDF of Rayleigh distribution can be described as [33]:

$$f_{(x)} = 1 - \exp\left(\frac{-x^2}{2\sigma^2}\right) \quad (9)$$

where x is the input (assuming it is an image). In this work, a modified gamma-adjusted Rayleigh distribution (MGARD) approach is introduced to control the visibility improvement level. The developed MGARD approach is computed as:

$$F_{(x,y)} = 1 - \left(\frac{-(K_{(x,y)})^2}{K_{(x,y)}}\right)^{\left(\frac{1}{\gamma}\right)} \quad (10)$$

According to Eq.10, $F_{(x,y)}$ is the MGARD output, and γ represents an adjustment factor accountable for the

enhancement level. With regards to γ , it must be as ($\gamma > 0$), wherein increasing its value causes luminance reduction and contrast increase. In addition, thorough tests showed that satisfactory results are gained if the value of γ is in the range of 0.1 to 0.5. These experiments have been performed on different nighttime images. At this point, image $F_{(x,y)}$ is enhanced but its pixels are not well-distributed over the entire dynamic range. Therefore, the automatic linear contrast stretching (ALCS) procedure is used to supply a natural range stretch by redistributing the pixel values to the entire interval. The following equation is utilized to compute the ALCS approach as [34]:

$$E_{(x,y)} = \alpha \cdot F_{(x,y)} - \beta \quad (11)$$

In Eq.11, the $E_{(x,y)}$ is the final processed value channel. The stretching elements α and β are used to determine the extent of stretch automatically as follows:

$$\alpha = \frac{1}{\max(F_{(x,y)}) - \min(F_{(x,y)})} \quad (12)$$

$$\beta = \frac{\min(F_{(x,y)})}{\max(F_{(x,y)}) - \min(F_{(x,y)})} \quad (13)$$

The *max* and *min* above represent the highest and lowest pixel values in $E_{(x,y)}$. Next, the color domain is converted back to the RGB domain as a final step of the proposed algorithm. Finally, the input of the developed algorithm is a nighttime image and γ , whereas the output is an illumination-enhanced image. The flowchart of the developed ASSR algorithm is demonstrated in Figure 5. Finally, Figure 6 displays the performance of ASSR with different γ values.

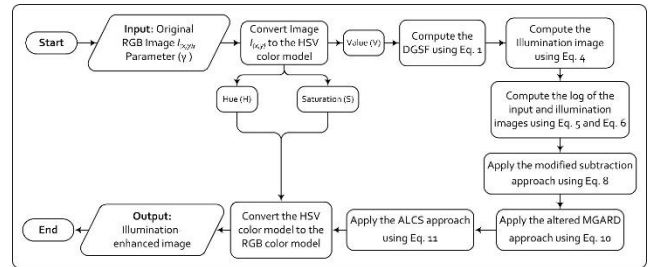


Fig. 5. Block diagram of the proposed ASSR algorithm.

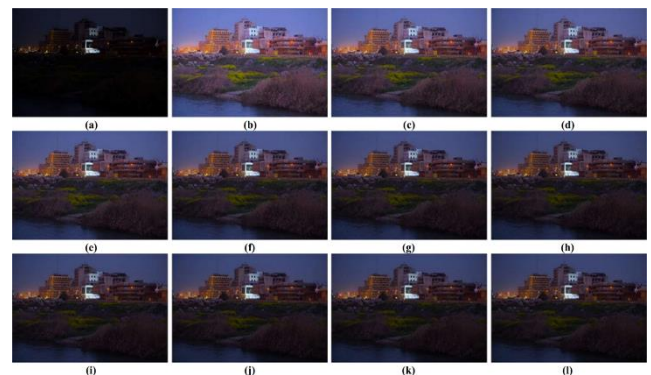


Fig. 6. Processing a nighttime image by the proposed algorithm: (a) degraded nighttime image captured by a Nikon D750 professional camera; the upcoming images are recovered with: (b) $\gamma = 0.1$, (c) $\gamma = 0.15$, (d) $\gamma = 0.2$, (e) $\gamma = 0.25$, (f) $\gamma = 0.3$, (g) $\gamma = 0.4$, (h) $\gamma = 0.55$, (i) $\gamma = 0.65$, (j) $\gamma = 0.7$, (k) $\gamma = 0.85$, (l) $\gamma = 1$.

IV. IMAGE EVALUATION METHODS

There are two basic methods of assessing image quality (IQ), which are subjective and objective. The subjective methods involve the opinions of the observers whereas the objective methods involve the computer algorithms. To accomplish an objective assessment, IQ metrics are used. The objective IQ metrics can be classified into full reference (FR), reduced reference (RR), and no reference (NR) metrics, in that these categories are based on information about the original image and the distortion process.

1. **FR IQ metrics:** measures the quality of a degraded or restored image depending on an ideal image.
2. **NR IQ metrics:** look only at the image under test and have no need for reference information.
3. **RR IQ metrics:** measures the quality of a restored image depending on a degraded image.

To objectively evaluate the outcomes of comparisons, three image evaluation methods were used, namely lightness order error (LOE) [35], blind multiple pseudo reference images (BMPRI) [36], and colorfulness (CFN) [37]. The LOE is a RR metric that is utilized to measure the error of illumination (i.e., naturalness) between the original image and its recovered counterpart [36]. The LOE metric is defined as:

$$LOE = \frac{1}{m * n} \sum_{i=1}^m \sum_{j=1}^n RD_{(i,j)} \quad (14)$$

Where m and n are the image dimensions and $RD_{(i,j)}$ is the relative order difference of the lightness between the degraded image and the enhanced one. The output for this metric is a numerical value, in that the smallest value indicates better natural illumination. The BMPRI is an NR metric that can be used to discover the quality of image details by introducing multiple pseudo reference images (MPRI) via increasing the distortions of the input image by applying several types of distortion aggravation during the MPRI generation to measure the possible distortions existing in the target image.

To further degrade the distorted image, four types of commonly encountered distortions are utilized to measure the blocking, ringing, blurring, and noising artifacts. For each type of distortion, five different levels are used. A total of twenty reference images are generated to give references of the same image content degraded by different distortions. Then, the local binary pattern features are extracted. After that, a comparison is made between

distorted images and MPRI to predict the final quality measure. The output for this metric is a numerical value, the smallest value indicates better visible details. Colorfulness (CFN) is the attribute of visual perception that the perceived color of an area appears to be somewhat chromatic. CFN is evoked by an object that depends not only on its spectral feature but also on the strength of the illumination. The CFN is an NR metric that measures the lucidity of colors depending on non-complex statistical approaches, as follows:

$$CFN = \sqrt{\sigma_{\alpha}^2 + \sigma_{\beta}^2} + 0.3\sqrt{\mu_{\alpha}^2 + \mu_{\beta}^2} \quad (15)$$

where $\alpha = R - G$, $\beta = (R + G)/2 - B$, and σ , μ are the standard deviation and the mean values of the image. The output for this metric is a numerical value, where the highest value indicates better colors.

V. RESULTS AND DISCUSSION

provided. The dataset includes more than 400 raw images captured by a Nikon D750 professional camera and a Samsung A70 smartphone camera. Moreover, different comparisons are made with various methods for subjective and objective evaluations. Likewise, discussions regarding the attained results of the aforesaid are provided. To demonstrate the filtering capabilities of the suggested algorithm, it is appraised against ten modern algorithms such as IMSR, PIE, FBE, CRM, LIME, LECARM, LightenNet, FOFM, AIE, and SDD. Figures 7-10 show the results of processing different real-degraded nighttime images by the developed algorithm.

In addition, Table 1 illustrates the recorded implementation times and evaluation values using three different image evaluation methods. Figures 11-13 demonstrate the comparison results, while Figures 14 -17 provide the average of recorded performances in Table 1 as charts. When applying the suggested algorithm to a set of nighttime images, it is observed that it was able to prevent the bright areas from becoming over-brightened and well-improved the illumination in the dark areas. Furthermore, the colors of the resulting images appear more natural, the contrast seems more vibrant, and the edges have acceptable sharpness. Likewise, no signs of visible processing defects appear on the results as they have an overall pleasant appearance. This indicates that the proposed algorithm has high capabilities to process different images taken by a professional camera or a smartphone. This is a true achievement as the proposed algorithm used non-complex computations when compared to other available algorithms to produce better-quality outcomes.



Fig. 7. Enhancing various real-degraded nighttime images captured by a Nikon D750 camera. (1st row) real nighttime images; (2nd row) images enhanced by the proposed algorithm.



Fig. 8. Enhancing various real-degraded nighttime images captured by a Nikon D750 camera. (1st row) real nighttime images; (2nd row) images enhanced by the proposed algorithm.



Fig. 9. Enhancing various real-degraded nighttime images captured by a Samsung A70 smartphone camera. (1st row) real nighttime images; (2nd row) images enhanced by the proposed algorithm.



Fig. 10. Enhancing various real-degraded nighttime images captured by a Samsung A70 smartphone camera. (1st row) real nighttime images; (2nd row) images enhanced by the proposed algorithm.



Fig. 11. Results obtained from comparing the proposed algorithm with different algorithms. (a1) Original nighttime image. The other images are recovered by: (a2) IMSR; (a3) PIE; (a4) FBE, (a5) CRM, (a6) LIME, (a7) LECARM, (a8) LightenNet, (a9) FOFM, (a10) AIE, (a11) SDD, (a12) Proposed algorithm.

Depending on the comparison results in Table 1 and Figure 11 to Figure 17, the illumination of all the resulting images has improved at different levels according to the utilized processing concept. All the comparison algorithms were able to increase the prominence of visible details in the murky regions of the degraded image and make them noticeable in the enhanced image. Moreover, many remarks were recorded related to the algorithms' performances, wherein they introduced either unwanted artifacts or failed in delivering adequate filtering for certain essential image traits such as colors, illumination, sharpness, or contrast. Accordingly, the IMSR algorithm showed certain latent image details and did not smooth the processed image. However, some drawbacks were noticed in its outcomes as they own insufficient illumination, improper contrast, and unnatural colors. Therefore, it recorded below high with LOE, the worst with CFN, and low with BMPRI. Still, it was the second-fastest among the comparative methods. The PIE algorithm the brightness of its results without introducing illumination errors as well as it did not introduce obvious smoothness. Therefore, it recorded the second-best in LOE. Still, both the color and visible quality of the resulting images did not get improved adequately. Thus, it recorded low scores with both CFN and BMPRI. The processing time was somewhat slow as it was recorded below moderate in such an aspect.



Fig. 12. Results obtained from comparing the proposed algorithm with different algorithms. (a1) Original nighttime image. The other images are recovered by: (a2) IMSR; (a3) PIE; (a4) FBE, (a5) CRM, (a6) LIME, (a7) LECARM, (a8) LightenNet, (a9) FOFM, (a10) AIE, (a11) SDD, (a12) Proposed algorithm.

The FBE algorithm yielded results with insufficient brightness. Thus, it recorded low readings with LOE. Besides, the sharpness was acceptable, but the colors were dimmed. Therefore, it recorded above low with CFN and high with BMPRI. It also provided reasonable implementation times as it recorded above moderate in this aspect. In addition, the images produced by the CRM algorithm have a dark look, faded colors, improper contrast, and no good visual detail, which is why it scored very low with LOE, very low with BMPRI, and above moderate with BMPRI, and above moderate implementation time.

As for the LIME algorithm, it is observed that it produced more impressive results compared with the aforesaid algorithms. It was very much close to the proposed algorithm in terms of CFN, BMITR, and processing times. Still, the LOE scores were the worst as LIME introduced different illumination errors. As for the LECARM algorithm, it was quite fast, but was not satisfactory on other metric scores, since the resulting images did not have sufficient illumination, the colors were unnatural, and some white shadows appeared on the significant edges of the resulting images. Thus, LECARM scored above low according to LOE, low according to CFN, and moderate according to BMPRI.



Fig. 13. Results obtained from comparing the proposed algorithm with different algorithms. (a1) Original nighttime image. The other images are recovered by: (a2) IMSR; (a3) PIE; (a4) FBE, (a5) CRM, (a6) LIME, (a7) LECARM, (a8) LightenNet, (a9) FOFM, (a10) AIE, (a11) SDD, (a12) Proposed algorithm.

The LightenNet algorithm recovered images with halo artifacts, dimmed areas, unsatisfactory illumination, and irregular color representation. Thus, it achieved below moderate with LOE, above moderate with CFN, and below moderate with BMPRI, as well it also provided low processing time. Additionally, the FOFM algorithm provided unusual performance as it introduced acceptable colors with extra smoothness, insufficient brightness, and improper contrast to the processed images. The visual details are not well-noticed due to the extra smoothness.

Therefore, it achieved moderately with LOE, very high with CFN, and worst according to BMPRI, as well it also provided very low processing time. The AIE on the other hand delivered dissimilar scores as the results appeared with insufficient contrast with apparent artifacts around the significant edges. Therefore, it recorded high with LOE, below high with CFN, and below high with BMPRI. It also provided above low processing times. The SDD algorithm was the slowest and did not provide enough illumination. The enhanced image suffers from increased smoothness, insufficient contrast, faded colors, and blurred visual details. Thus, it achieved above moderate with LOE, moderate with CFN, and very low according to BMPRI.

When it comes to the proposed algorithm, it scored the best in the aspects of visible quality, runtime, and image evaluation methods. Accordingly, it scored the best LOE, CFN, and BMPRI readings with the fastest runtime. Besides, its outputted images have innate illumination and contrast, proper colors, and preserved sharpness, achieving overall visually pleasing results. This is a considerable matter because it has a low computational cost and did not require numerous inputs to output its results.

Table 1. The recorded performances of the conducted comparisons.

Methods	Figure	LOE	CFN	BMPRI	Time/ sec.
IMSR	Fig 11	243.9704	14.4105	24.7731	0.404690
	Fig 12	373.2700	15.0104	16.2337	0.427745
	Fig 13	205.2676	17.6117	20.6682	0.618268
	Avg	<i>274.1693</i>	<i>15.6775</i>	<i>20.5583</i>	<i>0.4835</i>
PIE	Fig 11	180.7204	27.4046	20.2337	1.537313
	Fig 12	156.0939	29.0593	10.0268	1.345544
	Fig 13	132.5608	27.5972	19.6193	2.542043
	Avg	<i>156.4583</i>	<i>28.0203</i>	<i>16.6266</i>	<i>1.8083</i>
FBE	Fig 11	382.2822	29.8875	13.6589	0.800422
	Fig 12	795.9926	29.9789	10.1188	0.645618
	Fig 13	199.5464	30.9384	17.7982	0.871748
	Avg	<i>459.2737</i>	<i>30.2682</i>	<i>13.8586</i>	<i>0.7725</i>
CRM	Fig 11	341.4231	23.2571	15.2324	0.616634
	Fig 12	792.6087	24.4727	9.3880	0.552439
	Fig 13	270.9980	27.3672	17.4444	0.790295
	Avg	<i>468.3432</i>	<i>25.0323</i>	<i>14.0216</i>	<i>0.6531</i>
LIME	Fig 11	361.5281	39.1161	9.3429	0.427558
	Fig 12	766.8839	38.5640	10.0403	0.411701
	Fig 13	381.2160	39.8126	14.3225	0.523470
	Avg	<i>503.2093</i>	<i>39.1642</i>	<i>11.2352</i>	<i>0.4542</i>
LECARM	Fig 11	298.2141	26.0492	14.0215	0.469881
	Fig 12	742.7792	27.8017	10.5861	0.525108
	Fig 13	260.6524	28.5155	17.8083	0.650854
	Avg	<i>433.8819</i>	<i>27.4554</i>	<i>14.1386</i>	<i>0.5486</i>
LightenNet	Fig 11	260.1331	31.6785	18.2034	6.935749
	Fig 12	303.7097	36.2316	10.6206	7.060512
	Fig 13	663.2092	45.6496	15.3746	10.845192
	Avg	<i>409.0173</i>	<i>37.8532</i>	<i>14.7328</i>	<i>8.2804</i>
FOFM	Fig 11	304.7426	39.1554	18.3676	9.295876
	Fig 12	592.0673	36.4066	12.9458	10.354242
	Fig 13	310.4652	44.8257	33.7865	16.758153
	Avg	<i>402.4250</i>	<i>40.1292</i>	<i>21.6999</i>	<i>12.1360</i>
AIE	Fig 11	176.8957	38.2783	17.3501	3.147552
	Fig 12	311.8328	37.1978	10.7287	3.215684
	Fig 13	126.5756	38.9162	13.8414	3.441135
	Avg	<i>205.1013</i>	<i>38.1307</i>	<i>13.9734</i>	<i>3.2681</i>
SDD	Fig 11	246.0662	29.8299	28.4929	10.691191
	Fig 12	518.2903	30.4161	11.6166	9.078217
	Fig 13	277.5828	31.4161	24.3300	16.753891
	Avg	<i>347.3131</i>	<i>30.5540</i>	<i>21.4798</i>	<i>12.1744</i>
Proposed Algorithm	Fig 11	101.9926	43.5515	10.0828	0.092488
	Fig 12	181.6553	41.7961	9.0197	0.128568
	Fig 13	162.3424	46.0505	14.0314	0.137561
	Avg	<i>148.6634</i>	<i>43.7993</i>	<i>11.0446</i>	<i>0.1195</i>

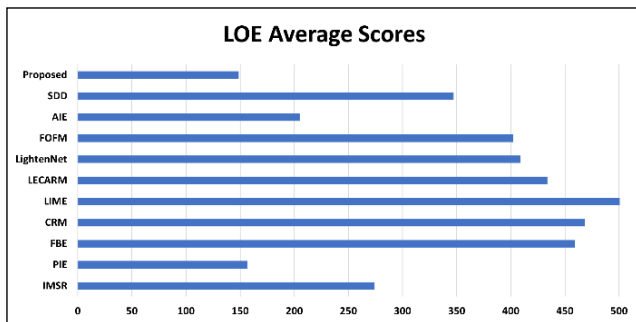


Fig. 14. Charts of the average LOE readings.

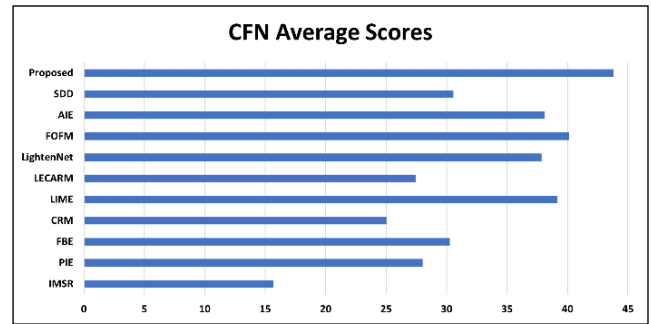


Fig. 15. Charts of the average CFN readings.

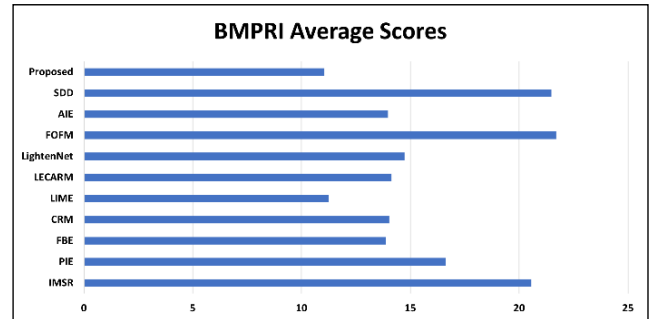


Fig. 16. Charts of the average BMPRI readings.

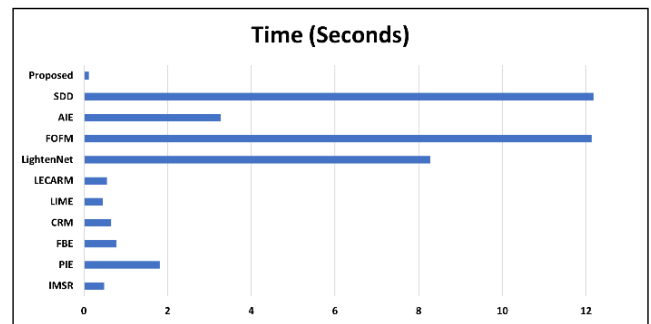


Fig. 17. Charts of the average runtimes.

VI. CONCLUSION

This research introduced an adapted SSR algorithm for nighttime images, as the standard SSR algorithm did not process such images adequately. The adaption is made by working in the HSV color domain, applying some adjustments including a modified subtraction process with two further processing steps to improve the illumination and contrast. The developed ASSR algorithm has been tested extensively with numerous raw images obtained from a Nikon D750 camera and a Samsung A70 smartphone. As for the experiments, the obtained results were promising as when the processed images are compared with their unprocessed versions, the processing ability of the developed ASSR can be seen as its outputs own satisfactory illumination, adequate colors, and proper contrast. In addition, it can be observed that the bright areas were preserved, and the darkened areas were improved without smoothing the results or generating undesirable filtering

flaws. As for the companions, subjective and objective evaluations revealed that the performance of the developed ASSR algorithm surpassed many existing algorithms when it comes to the overall appearance, recorded accuracies, and processing speed. This is a true accomplishment as carefully introducing modifications to the SSR algorithm led to the production of a simple structure algorithm with low computations that can achieve impressive results. In future work, extra modifications can be made to the ASSR algorithm such as complete processing automation.

Acknowledgment

The authors are thankful to the Department of Computer Science, at the University of Mosul for their assistance that contributed to the achievement of this research.

References

- [1] A. Yamasaki, T. Kanade, H. Takauji, H. Ohki, and S. Kaneko, "Denight: Nighttime image enhancement using daytime image," *IEEE Trans. Electron. Inf. Syst.*, vol. 129, no. 12, pp. 2222–2231, 2009.
- [2] A. S. Parihar and K. Singh, "A study on Retinex based method for image enhancement," in *2018 2nd International Conference on Inventive Systems and Control (ICISC)*, 2018.
- [3] Y. Zhou, C. Shi, B. Lai, and G. Jimenez, "Contrast enhancement of medical images using a new version of the World Cup Optimization algorithm," *Quantitative Imaging in Medicine and Surgery*, vol. 9, no. 9, pp. 1528–1547, 2019.
- [4] J. Dadwal, and B. Sharma, "Design of image processing technique in digital enhancement application," *Asian Journal of Applied Science and Technology*, vol. 1, no. 1, p. 3-5, 2017.
- [5] X. Jiang, H. Yao, and D. Liu, "Nighttime image enhancement based on image decomposition," *Signal Image Video Process.*, vol. 13, no. 1, pp. 189–197, 2019.
- [6] K. Zhou, C. Jung, and S. Yu, "Scale-aware multispectral fusion of RGB and NIR images based on alternating guidance," *IEEE Access*, vol. 8, pp. 173197–173207, 2020.
- [7] J. Wei, Q. Zhijie, X. Bo, and Z. Dean, "A nighttime image enhancement method based on Retinex and guided filter for object recognition of apple harvesting robot," *International Journal of Advanced Robotic Systems*, vol. 15, no. 1, pp. 1-12, 2018.
- [8] S. Wang, J. Zheng, and B. Li, "Parameter-adaptive nighttime image enhancement with multi-scale decomposition," *IET Computer Vision*, vol. 10, no. 5, pp. 425–432, 2016.
- [9] P. Tao, H. Kuang, Y. Duan, L. Zhong, and W. Qiu, "BITPNet: Unsupervised bio-inspired two-path network for nighttime traffic image enhancement," *IEEE Access*, vol. 8, pp. 164737–164746, 2020.
- [10] Z. Shi, M. M. Zhu, B. Guo, M. Zhao, and C. Zhang, "Nighttime low illumination image enhancement with single image using bright/dark channel prior," *EURASIP Journal on Image and Video Processing*, vol. 2018, no. 1, pp 1-15, 2018.
- [11] Y. Yang, Z. Jiang, C. Yang, Z. Xia, and F. Liu, "Improved retinex image enhancement algorithm based on bilateral filtering," in *Proceedings of the 4th International Conference on Mechatronics, Materials, Chemistry and Computer Engineering 2015*, 2015.
- [12] J. Ma, X. Fan, J. Ni, X. Zhu, and C. Xiong, "Multi-scale retinex with color restoration image enhancement based on Gaussian filtering and guided filtering," *International Journal of Modern Physics B*, vol. 31, no. 16–19, p. 1744077, 2017.
- [13] H. Lin and Z. Shi, "Multi-scale retinex improvement for nighttime image enhancement," *Optik*, vol. 125, no. 24, pp. 7143–7148, 2014.
- [14] X. Fu, Y. Liao, D. Zeng, Y. Huang, X.-P. Zhang, and X. Ding, "A probabilistic method for image enhancement with simultaneous illumination and reflectance estimation," *IEEE Transactions on Image Processing*, vol. 24, no. 12, pp. 4965–4977, 2015.
- [15] X. Fu, D. Zeng, Y. Huang, Y. Liao, X. Ding, and J. Paisley, "A fusion-based enhancing method for weakly illuminated images," *Signal Processing*, vol. 129, pp. 82–96, 2016.
- [16] Z. Ying, G. Li, Y. Ren, R. Wang, and W. Wang, "A new low-light image enhancement algorithm using camera response model," in *2017 IEEE International Conference on Computer Vision Workshops (ICCVW)*, 2017.
- [17] X. Guo, Y. Li, and H. Ling, "LIME: Low-light image enhancement via illumination map estimation," *IEEE Transactions on Image Processing*, vol. 26, no. 2, pp. 982–993, 2016.
- [18] Y. Ren, Z. Ying, T. H. Li, and G. Li, "LECARM: Low-light image enhancement using the camera response model," *IEEE Transactions on Circuits and Systems for Video Technology*, vol. 29, no. 4, pp. 968–981, 2019.
- [19] C. Li, J. Guo, F. Porikli, and Y. Pang, "LightenNet: A Convolutional Neural Network for weakly illuminated image enhancement," *Pattern Recognition Letters*, vol. 104, pp. 15–22, 2018.
- [20] Q. Dai, Y.-F. Pu, Z. Rahman, and M. Aamir, "Fractional-order fusion model for low-light image enhancement," *Symmetry*, vol. 11, no. 4, pp. 1-17, 2019.
- [21] W. Wang, Z. Chen, X. Yuan, and X. Wu, "Adaptive image enhancement method for correcting low-illumination images," *Information Sciences*, vol. 496, pp. 25–41, 2019.
- [22] S. Hao, X. Han, Y. Guo, X. Xu, and M. Wang, "Low-light image enhancement with semi-decoupled decomposition," *IEEE Transactions on Multimedia*, vol. 22, no. 12, pp. 3025–3038, 2020.
- [23] W. Huang, Y. Zhu, and R. Huang, "Low light image enhancement network with attention mechanism and retinex model," *IEEE Access*, vol. 8, pp. 74306–74314, 2020.
- [24] Y. Yang, Z. Jiang, C. Yang, Z. Xia, and F. Liu, "Improved retinex image enhancement algorithm based on bilateral filtering," in *Proceedings of the 4th International Conference on Mechatronics, Materials, Chemistry and Computer Engineering 2015*, 2015.
- [25] A. M. Gonzales and A. M. Grigoryan, "Fast Retinex for color image enhancement: methods and algorithms," in *Mobile Devices and Multimedia: Enabling Technologies, Algorithms, and Applications 2015*, 2015.
- [26] Z. Al-Ameen and G. Sulong, "A new algorithm for improving the low contrast of computed tomography images using tuned brightness controlled single-scale retinex," *Scanning*, vol. 37, no. 2, pp. 116–125, 2015.
- [27] Y. Wu, W. Song, J. Zheng, and F. Liu, "A new low light image enhancement based on the image degradation model," in *2018 14th IEEE International Conference on Signal Processing (ICSP)*, 2018.
- [28] K. Singh and A. Parihar, "A comparative analysis of illumination estimation-based Image Enhancement techniques," in *2020 International Conference on Emerging Trends in Information Technology and Engineering (ic-ETITE)*, 2020.
- [29] N. Faraj and L. Abood, "Single scale retinex (SSR) and multi scale retinex (MSR) enhancement algorithms for thermal night-vision images," *Iraqi Journal of Science*, vol. 58, no. 4C, 2017.
- [30] A. Zotin, "Fast algorithm of image enhancement based on multi-scale retinex," *Procedia Computer Science*, vol. 131, pp. 6–14, 2018.
- [31] L. Navarro, G. Deng, and G. Courbebaïsse, "The symmetric logarithmic image processing model," *Digital Signal Processing*, vol. 23, no. 5, pp. 1337–1343, 2013.
- [32] A. S. Abdul Ghani and N. A. Mat Isa, "Underwater image quality enhancement through integrated color model with Rayleigh distribution," *Applied Soft Computing*, vol. 27, pp. 219–230, 2015.
- [33] G. Wang, Q. Dong, Z. Pan, X. Zhao, J. Yang, and C. Liu, "Active contour model for ultrasound images with Rayleigh distribution," *Mathematical Problems in Engineering*, vol. 2014, pp. 1–12, 2014.
- [34] Z. Al-Ameen, "Satellite image enhancement using an ameliorated balance contrast enhancement technique," *Traitement du Signal*, vol. 37, no. 2, pp. 245–254, 2020.

- [35] S. Bao, S. Ma, and C. Yang, "Multi-scale retinex-based contrast enhancement method for preserving the naturalness of color image," Optical Review, vol. 27, no. 6, pp. 475–485, 2020.
- [36] X. Min, G. Zhai, K. Gu, Y. Liu, and X. Yang, "Blind image quality estimation via distortion aggravation," IEEE Transactions on Broadcasting, vol. 64, no. 2, pp. 508–517, 2018.
- [37] S. E. Susstrunk and S. Winkler, "Color image quality on the Internet," in Internet Imaging V, 2003.

تكيف خوارزمية الرتينكس ذات المقياس الواحد لتحسين الصور الليلية

زهير الأمين محمد خليل اسماعيل
qizohair@uomosul.edu.iq

قسم علوم الحاسوب، كلية علوم الحاسوب والرياضيات
جامعة الموصل، الموصل، نينوى، العراق

تاريخ استلام البحث: 2021/10/24 تاريخ قبول البحث: 2021/11/29

الخلاصة:

تملك الصور الملتقطة ليلاً في ظروف الإضاءة المنخفضة تفاصيل مرئية مفقودة، تباين غير كافي، سطوح منخفضة وضوضاء. لذلك، من الصعب إدراك واستخراج وتحليل المعلومات المرئية المهمة من هذه الصور ما لم تتم معالجتها بشكل صحيح. توجد خوارزميات مختلفة لمعالجة الصور الليلية، ومع ذلك، فإن معظم هذه الخوارزميات معقدة، وتنتج عيوب معالجة، وتفرض في تعميم الصور، أو لا تحسن الإضاءة بشكل كافٍ. وبالتالي، تم تكيف خوارزمية الرتينكس ذات المقياس الواحد في هذه الدراسة لتوفير معالجة أفضل للصور الليلية. تبدأ الخوارزمية المقترحة بتحويل الصورة الملونة من نموذج RGB إلى نموذج HSV وتحسين قناة V فقط مع الحفاظ على قنوات H و S. بعد ذلك، يتم تحديد النسخة المضئية للصورة، وتحسب لوغاريتمات الصور المضئية والأصلية، ثم تطرح هاتين الصورتين باستخدام طريقة معدلة. بعد ذلك، يتم تطبيق دالة توزيع Rayleigh المعدلة بضبط كاما، وتتم معالجة نتيجتها مرة أخرى من خلال طريقة تمدد التباين الخطي التلقائي لإنتاج قناة V المعالجة التي سيتم استخدامها مع قنوات H و S المحفوظة لتوليد صورة RGB الناتجة. تم تقييم الخوارزمية المطورة باستخدام مجموعة صور حقيقية ليلية، ويتم تقييمها باستخدام ثلاث طرق مخصصة للصور، ومقارنتها بعشر خوارزميات مختلفة وحديثة. أظهرت النتائج المتحصل عليها أن الخوارزمية المقترحة يمكنها تحسين الجودة البصرية للصور الليلية بشكل كبير بسرعة وكفاءة مع منع ظهور عيوب المعالجة، بالإضافة إلى إظهار القدرة على تجاوز أداء الخوارزميات الموجودة المختلفة بشكل ملحوظ.

الكلمات المفتاحية: تحسين الصور، الصورة الليلية، ريتينكس بمقياس واحد، الأساليب الإحصائية، SSR، HSV.